

**Inhibition of c-Myc down-regulation by sustained ERK
activation prevents the antimetabolite methotrexate- and
gemcitabine-induced differentiation in non-small cell lung
cancer cells**

Jordi M. Serra[†], Antonio Gutiérrez, Regina Alemany[†], María Navarro, Teresa Ros,
Carlos Saus, Jordi Ginés, Antonia Sampol, Juan Carlos Amat, Lorenzo Serra-Moisés,
Javier Martín, Antonio Galmés, Oliver Vögler, Joan Besalduch.

Department of Hematology, Institut Universitari d'Investigacions en Ciències de la
Salut (IUNICS), University Hospital Son Dureta, Palma de Mallorca, Spain (J.M.S.,
A.G., M.N., A.S., J.C.A., A.G., J.B); Group of Clinical and Molecular Onco-
Hematology, Department of Biology, University of the Balearic Islands, Palma de
Mallorca, Spain (J.M.S., A.G., R.A., T.R., L. S.-M., J.M., O.V.); Department of
Pathology (C.S.); Department of Pharmacy (J.G.); Department of Oncology (J.M)
University Hospital Son Dureta, Palma de Mallorca, Spain.

Running title: Sustained ERK activation inhibits differentiation via c-Myc

(†)Corresponding Authors:

Jordi M. Serra, Department of Hematology, Institut Universitari d'Investigacions en Ciències de la Salut (IUNICS), University Hospital Son Dureta, c/Andrea Dòria 55, E-07014 Palma de Mallorca, Spain; Tel.: +34 971-175155; Fax: +34 971-175360; E-mail: jmserra@hsd.es

Regina Alemany, Group of Clinical and Molecular Onco-Hematology, Department of Biology, University of the Balearic Islands, Ctra. Valldemossa Km 7.5, E-07122 Palma de Mallorca, Spain; Tel: +34 971-259619; Fax: +34 971 173184; E-mail: regina.alemany@uib.es

Number of text pages:	29
Number of tables:	0
Number of figures:	7
Number of references:	29
Number of words <i>Abstract</i> :	234 words
Number of words <i>Introduction</i> :	670 words
Number of words <i>Discussion</i> :	1478 words

Nonstandard abbreviations:

MTX – methotrexate; ERK – extracellular signal-regulated kinase; GE – gemcitabine

ABSTRACT

Non-small cell lung cancer (NSCLC) is characterized by severe resistance to chemotherapy. Here, we demonstrate that A549 adenocarcinoma cells permanently differentiate with the antimetabolites, methotrexate (MTX) and gemcitabine (GE), when blocking the antitumoral resistance mechanism that normally counteracts this process. MTX (1-10 μ M) and GE (1 μ M) induced growth arrest accompanied by sustained ERK1/2 phosphorylation and moderate reduction of c-Myc levels after 96 h, while only a low percentage of the cells differentiated. Combination with the MEK inhibitor U0126 reduced MTX- or GE-induced ERK1/2 over-phosphorylation and nearly abolished c-Myc expression, while provoking radical morphological changes in all cells. Besides the appearance of multilamellar bodies and intracellular cytokeratine reorganization, modulation of molecular markers occurred in a manner consistent with differentiation (gelsolin +300%; surfactant protein A and C -70%). Similar to U0126, c-Myc inactivation with specific siRNA initiated differentiation only in the presence of MTX, demonstrating that inhibition of the MAPK/ERK pathway alone or downregulation of c-Myc are not sufficient to induce this process. Importantly, withdrawal of antitumoral drugs and U0126 neither reversed differentiation nor reactivated proliferation. Our results reveal that maintenance of a certain threshold of c-Myc expression through sustained ERK1/2 activation represents a molecular mechanism that confers resistance to antimetabolite-induced differentiation in A549 cells, and provide a novel molecular basis for therapeutic strategies based on irreversible differentiation of cancer cells using conventional chemotherapeutic antimetabolites in combination with inhibitors of the MEK/ERK pathway or c-Myc.

INTRODUCTION

The failure of the delicate balance between cell proliferation, apoptosis and differentiation is normally associated with the development of cancer. Among the different classes of cancer, lung cancer currently [MSOffice1] represents the leading cause of cancer mortality in men and women, and within this group pulmonary adenocarcinoma is one of the most common types (Moran, 2006). Surgical resection of these tumors may be an effective treatment for stage I or stage II [MSOffice2] lung cancer, but many patients are diagnosed with advanced disease, where surgical cures are ineffective (Maghfoor and Perry, 2005) and make classical chemotherapeutic agents an unavoidable adjuvant treatment. Nevertheless, the most commonly used antineoplastic drugs in lung cancer, especially in non-small cell lung cancer (NSCLC) (e.g. gemcitabine, cisplatin, paclitaxel, among others), are associated with high rates of drug resistance and low disease-free survival periods making this cancer an incurable disease. Although there have been many efforts to overcome multidrug resistance, few significant advances have been made. Moreover, the role of the different forms and molecular mechanisms involved in drug resistance in lung cancer is complex and only partially understood (d'Amato et al., 2007).

Likewise, tumor cells are able to resist the cytotoxic effects of chemotherapy by achieving a quiescent, non-proliferating state that can be reversed after a variable period [MSOffice3], thus resulting in treatment failure. A novel therapeutic approach aimed at controlling the tumoral cells that resist chemotherapy, is based on the induction of cancer cell differentiation. The so-called “differentiation therapy” is an emergent area in cancer research and involves the reversion of a cancer cell to a more mature phenotype with no proliferative potential (Marchal et al., 2006). Several compounds such as butyrates, retinoids, and Vitamin D are able to induce differentiation in colon and other

cancer cells (Spira and Carducci, 2003). In this context, it has been demonstrated that certain chemotherapeutic antimetabolites, such as folate analog methotrexate (MTX) and deoxycytidine analog gemcitabine (GE) (2',2'-difluorodeoxycytidine), besides blocking cell proliferation, have a certain potential to induce differentiation in various human cancer cell lines (Bierau et al., 2006; Kimura et al., 2004; Singh et al., 2006). Both these properties were mainly attributed to its inhibitory effect on purine and pyrimidine biosynthesis and DNA synthesis.

A pivotal pathway related to differentiation of cells, as well as many other cellular functions, such as proliferation, survival and development, is the mitogen-activated protein kinase (MAPK) pathway composed of three subfamilies: extracellular signal-regulated kinase (ERK), p38 MAPK, and c-jun N-terminal kinase (JNK) (Nishimoto and Nishida, 2006; Seger and Krebs, 1995). The ERK subfamily of MAP kinases promotes cellular survival by successive phosphorylation of mitogen-activated protein kinase/ERK kinase (MEK), ERK, and downstream substrates such as Elk-1 and p90RSK. Moreover, ERK is implicated in the regulation of the transcription factor c-Myc, a nuclear protein blocking cell differentiation, including several types of cancer cells (Chen et al., 2006; Vita and Henriksson, 2006). In this context, it has been very recently discussed^[MSOffice4] that inhibition of this MAPK pathway could be a novel target for antitumoral treatments (Kohno and Pouyssegur, 2006).

We have recently observed that treatment with the antimetabolites MTX or GE induced a sustained phosphorylation of ERK1/2 in non-small cell lung cancer (NSCLC) A549 cells. Surprisingly, most of the treated cells were nevertheless found in a non-proliferative and also non-differentiated state of the cell cycle, known as quiescent or G0/G1. Taking these observations as a starting point we demonstrated that A549 cells can revert their neoplastic characteristics and differentiate under MTX and GE

treatment, but only when the accompanying ERK/c-Myc pathway activation is inhibited. For this reason, sustained activation of the ERK pathway must be considered as an antitumoral drug resistance mechanism, avoiding differentiation of the MTX- and GE-treated NSCLC A549 cells by stabilizing c-Myc levels. To extend the knowledge about the molecular mechanism(s) involved in this type of antitumoral resistance is of great clinical relevance, because it would allow the design of new therapeutical strategies based on the use of conventional chemotherapeutic agents, such as antimetabolites (e.g., MTX and GE) in combination with inhibitors of the MAPK pathway.

MATERIALS AND METHODS

Cell Culture and treatments – A549 human lung adenocarcinoma cells were obtained from the American Type Culture Collection (Manassas, VA). The cells were grown in RPMI 1640 medium supplemented with 2 mM glutamine, 10% (v/v) fetal calf serum, 100 units/ml penicillin, 100 µg/ml streptomycin, and 0.25 µg/ml amphotericin B in 5% CO₂. Tissue culture medium and supplements were all purchased from Sigma (Madrid, Spain). When the cells reached 60-70% confluence, vehicle (control), methotrexate (MTX; ((S)-2-(4-(((2,4-diaminopteridin-6-yl)methyl)(methyl)amino)benzamido)pentanedioic acid) (0.1–10 µM), gemcitabine (GE; 4-amino-1-[3,3-difluoro-4-hydroxy-5-(hydroxymethyl)tetrahydrofuran-2-yl]-1H-pyrimidin-2-one) (0.1-1 µM), U0126 (10 µM) (MEK inhibitor) (Cell Signaling Technology, Beverly, MA), or their combinations were added to the medium for 24 or 96 h. After the incubation period, the cell monolayers were twice washed with phosphate-buffered saline (PBS), cell attachment was disrupted with a trypsin-EDTA treatment (0.05% trypsin plus 0.08% EDTA in PBS) for 5 min at 37 °C for cell counting and cell cycle analysis or with a rubber policeman for immunoblotting, and the cells were resuspended in the appropriate buffer (see the corresponding sections).

Cell cycle analysis – Analysis of the cell cycle by flow cytometry was performed on A549 cells as previously described (Martinez et al., 2005a). Cell populations in the different phases of the cell cycle (sub-G1, G0/G1, S, and G2/M) were determined based on their DNA content in a Beckman Coulter Epics XL flow cytometer.

Gene silencing by small interfering RNA (siRNA) transfection – A549 cells were transfected with validated siRNA duplex oligos targeting human c-Myc mRNA (5 nM) (Catalog n° 6341; Cell Signaling Technology, Beverly, MA) by using Hyperfect transfection reagent (Qiagen) according to the manufacturer's instructions. Briefly, 1.5

μl of siRNA (2 μM stock concentration) was incubated in the presence of 3 μl of Hyperfect transfection reagent in 100 μl of serum-free RPMI 1640 medium plus antibiotics/antimycotics. After 10 min of incubation to allow the formation of transfection complexes, A549 cells ($0,5 \times 10^5$ cells) resuspended in 500 μl of RPMI medium (containing serum and antibiotics/antimycotics) were mixed with the siRNA-Hyperfect reagent transfection complexes or with Hyperfect reagent alone (Mock) into the well, and incubated for 48 h. After this time, vehicle (siRNA c-Myc) or 10 μM MTX (siRNA c-Myc + MTX) was added to the cells and incubated for an additional 96 h.

Immunoblot analysis – Preparation of cell extracts, protein assays, and quantitative immunoblotting were performed as previously described (Martinez et al., 2005b) with the following change, sodium orthovanadate and cantharidin were both added to the ice-cold lysis buffer at the final concentration of 1 μM . Quantification was performed by image analysis, using standard curves with four points (i.e., total protein loaded vs. integrated optical density) of different protein contents loaded on the same gel as described (Martinez et al., 2005b). Primary polyclonal antibodies, anti-poly ADP-ribose polymerase (anti-PARP, diluted 1:1000), anti-phospho-p44/42 MAP kinase (P-ERK1/2) (Thr202/Tyr204) (diluted 1:1000), anti-p44/42 MAP kinase (ERK1/2) (diluted 1:1000) and anti-c-Myc (diluted 1:500) (70 kDa) were obtained from Cell Signaling Technology (Beverly, MA). Primary monoclonal anti-gelsolin (93 kDa) was from BD Biosciences Transduction Laboratories (Heidelberg, Germany), whereas polyclonal anti-surfactant protein A (SP-A) (35 kDa) and protein C (SP-C) (precursor SP-C 21 kDa) antibodies were from Santa Cruz Biotechnology, Inc. (USA).

Quantitative reverse transcription-polymerase chain reaction (RT-PCR) of ERK1 mRNA expression. Total RNA was isolated from 5×10^5 A549 cells with TRIzol reagent

(Invitrogen, Carlsbad, CA, USA) according to the manufacturer's instructions. Primer design and optimization was carried out using the Biology WorkBench (<http://workbench.sdsc.edu>) and the Oligoanalyzer program (Integrated DNA Technologies, Coralville, IA) and resulted in the following sequences: ERK1: forward 5'-ACTATGACCCGACGGATGAG-3', reverse 5'-CTAACAGTCTGGCGGGAGAG - 3; β -Glucuronidase (GUS): forward 5'-GAAAATATGTGGTTGGAGAGCTCATT-3', reverse 5'-CCGAGTGAAGATCCCCTTTTTA-3'. Real-time PCR quantification was performed using the LightCycler System (Roche Diagnostics) including a melting curve analysis of the final products. Expression results were normalized according to the housekeeping gene expression (β -Glucuronidase).

Immunocytochemistry detection of cytokeratine and ki-67 – Immunohistochemistry of cytokeratine (Ck) (Cam 5.2) and ki-67 was carried out on A549 cells fixed with 4% paraformaldehyde overnight at room temperature. The cells were incubated with anti-cytokeratine (Neo-markers, Fremont, CA, USA) and anti-Ki-67 (Santa Cruz Biotechnology, Inc., USA) antibodies at dilution of 1:100 for 1 h at room temperature. Detection was performed with avidin/oxidase complex, according to the manufacturer's instructions (Vectastain ABC kit; Vector Laboratories, Burlingame, CA, USA). Negative control slides were only exposed to secondary antibodies. Cells were counterstained with haematoxylin, dehydrated, and mounted for conventional microscopy.

Ultrastructural study - A549 cells were fixed in 4% glutaraldehyde in 0.1 M sodium cacodylate buffer, postfixed with aqueous 1.25% osmium tetroxide, stained with 4% aqueous uranyl acetate, dehydrated in a graded ethanol series, and embedded in Polybed (epoxy resin). An ultramicrotome (Reichert-Jung Ultra Cut) was used to prepare ultrathin sections of the cells, which were then double-stained with uranyl acetate and

lead citrate. The sections were then observed using a transmission electron microscope (Zeiss 902 electron microscope) with an acceleration voltage of 100 kV. All reagents for electron microscopy were purchased from Electron Microscopy Sciences (Ft. Washington, PA) except Polybed (Polysciences, Warrington, PA).

Cell proliferation assays – To study the effect of the withdrawal of MTX, GE or MTX, GE plus U0126 on cell proliferation, cells were recovered after treatment with vehicle (control), MTX (0.1 and 10 μ M), GE (0.1 and 1 μ M) or the combination MTX or GE and U0126 (10 μ M) for 96 h, diluted and reseeded at a density of 10 cells per well in 24-well plates with 0.5 ml of culture medium. At the end of ten and twenty days of cell culture, cells were counted using an automated cell counter (Advia 120; Bayer Diagnostics, Tarrytow, NY).

Data analysis – The results are expressed as the mean \pm S.E.M. of at least three independent experiments. The Student's *t*-test or one-way Anova (where indicated) followed by Tukey's test was used for statistical evaluations. Differences were considered statistically significant at $P < 0.05$.

RESULTS

As the antifolate, methotrexate (MTX), is known to inhibit cell proliferation, we evaluated the effect of 24 h MTX treatment on the cell cycle of A549 lung adenocarcinoma cells in serum-containing medium by flow cytometry. MTX treatment (10 μ M for 24 h) inhibited proliferation of NSCLC A549 cells and induced a significant increase of 41 ± 3 % in the number of cells in G0/G1 phase, with a simultaneous decrease of 43 ± 3 % in the cell population in S and G2 (Fig. 1B and C). As expected, in vehicle-treated cells (control) a higher percentage of cells, $49 \pm 1\%$, was found in the S/G2/M phase of cell cycle (Fig. 1A and C). Similar results were obtained after treatment with 1 μ M MTX for 24 h (data not shown). Moreover, no significant sub-G1 population, a peak that is associated with apoptosis, could be detected. Accordingly, no PARP fragmentation was induced by this treatment (Fig. 1D). These data suggest that MTX treatment inhibited cell proliferation by impairing cell cycle progression through the G1 checkpoint, without inducing apoptosis in A549 cells. Moreover, we observed that a small fraction of A549 cells changed their morphological appearance to a more epithelial-like cell type after long-term treatment (96 h) with 10 μ M MTX (see Figure 6B).

We next determined the activation status of ERK1/2, a central component of the MAPK pathway involved in cell proliferation, survival and differentiation, by immunodetection. Although MTX inhibited A549 cell proliferation, the phosphorylation levels of ERK1/2 were drastically increased after treatment with MTX at 1 and 10 μ M for 24 h, being about four to six fold of that of control cells (Fig. 2A). Activation of ERK1/2 was sustained, since its phosphorylation was still elevated after 96 h of treatment, without affecting total ERK expression (Fig. 2A, B). Additionally, 96 h treatment with the nucleoside analog gemcitabine (GE, 1 μ M), an effective established

agent in the treatment of NSCLC, also induced sustained ERK1/2 activation as MTX did (Fig. 2B). When A549 cells were incubated with vehicle, MTX (10 μ M) or GE (1 μ M) in combination with the MEK inhibitor U0126 (10 μ M) for 96 h a pronounced decline of basal- and drug-induced phosphorylation of ERK1/2 levels was observed. U0126 treatment diminished by $59 \pm 6\%$ and $76 \pm 4\%$ basal phosphorylation of ERK1 and 2 (Fig. 2B). Moreover, combination of U0126 with antimetabolites decreased by around 51% and 40% MTX- and GE-induced phosphorylation of both ERK proteins, respectively, suggesting that MEK activation is implicated in antimetabolite-induced ERK phosphorylation (Fig. 2B). Total ERK1/2 expression remained unchanged after 96 h treatment with MTX, GE, U0126 or their combination (Fig. 2B).

We next set out to analyze whether the total cellular level of the transcription factor c-Myc, a down-stream target of the MEK/ERK pathway, was also influenced by these antimetabolites. Although MTX (10 μ M) and GE (1 μ M) treatments for 96 h induced sustained phosphorylation of ERK1/2, they decreased total c-Myc protein levels by $42.5 \pm 5.4\%$ and $65.9 \pm 8.1\%$, respectively (Fig. 2B). Still, combination of MTX or GE and U0126 (10 μ M) further decreased by 1.81 and 1.27 fold the MTX- and GE-induced reductions of c-Myc protein levels, leading to a total decrease of about 82%, compared with vehicle-treated cells (Fig. 2B). The effect of the inhibition of ERK phosphorylation on proliferation and phenotype alterations in vehicle- and antimetabolite-treated A549 cells was then studied. As found with MTX (10 μ M) or GE (1 μ M) alone, both antimetabolites in combination with U0126 (10 μ M) for 96 h also inhibited cell proliferation (inhibition of 19%, 95% and 94% with U0126, MTX or GE alone and 92 % with MTX or GE plus U0126, compared with vehicle-treated cells), which was additionally confirmed by immunocytochemistry evaluating the level of the nuclear factor ki-67. Expression of nuclear factor ki-67, commonly associated with

increased proliferation, decreased in cells treated with MTX alone or in combination with U0126, compared to vehicle- or U0126-treated cells (data not shown). In particular, MTX or GE in combination with U0126 induced the ubiquitous emergence of a morphological cell phenotype similar to an epithelial cell, with a more abundant, flattened cytoplasm and increased cytoplasmic:nuclear ratio. The analysis of several proteins considered to be molecular markers of cell differentiation was performed to determine whether these morphological changes were signs of differentiation. Taking into account that lung tissue is usually composed of various epithelial cell lineages, and that no collectively valid marker for the differentiated state of these cells has so far been described, we examined the general differentiation marker gelsolin (Hoshikawa et al., 1994) and the specific markers of undifferentiated progenitor lineage for the pulmonary alveolar epithelium (i.e., type II pneumocytes), surfactant protein A (SP-A) and C (SP-C) (Betz et al., 1995). The cellular levels of gelsolin in A549 cells treated with MTX (10 μ M) or U0126 (10 μ M) for 96 h were moderately augmented by 76 and 81%, respectively, compared with the control cells. However, the combination of MTX and U0126 dramatically increased the level of this differentiation marker four fold (Fig. 3A). Similar to MTX, treatment with GE (1 μ M) for 96 h increased the level of gelsolin four fold, whereas its combination with U0126 further increased the expression of this protein by 25%. Furthermore, the SP-A and SP-C markers decreased in growth arrested A549 cells treated with MTX (reduction of 31% and 46%, respectively) and GE (reduction of 42% and 66%, respectively) alone and further down-regulated in combination with U0126 (reduction of 48% and 59% with MTX plus U0126 and 69% and 85% with GE plus U0126, respectively), compared with vehicle-treated cells (Fig. 3B and C). Finally, ultrastructural studies by electron microscopy showed that combination of MTX and U0126 induced the appearance of cytoplasmic multilamellar

bodies (myelinosomes) (Fig. 4), typical secretory granules in normal type II alveolar epithelium cells, which were not observed in vehicle- and only singularly detectable in MTX-treated cells (Fig. 4). This inverse relation is probably caused by the fact, that in differentiated cells the production of both surfactant proteins occurs in a more organized way. Therefore, delocalized high level expression of these proteins might be stopped and replaced by a structured physiological production, restricted to myelinosomes. Together, these data suggest that sustained ERK1/2 phosphorylation in cell growth arrested A549 cells impaired MTX- and GE-induced cell differentiation, most probably by maintaining a certain level of c-Myc expression.

To corroborate that maintenance of c-Myc expression by sustained ERK1/2 phosphorylation prevents these cells from MTX-induced differentiation, A549 cells were transiently transfected with a small interfering (Si) RNA against c-Myc for 48 h, and then for an additional 96 h with 10 μ M MTX. As expected, siRNA c-Myc transfected A549 cells expressed reduced levels of c-Myc protein at the end of treatment (reduction of 47%), and a concomitant increase of ERK1/2 phosphorylation (increase of $354 \pm 52\%$ and $221 \pm 51\%$ in P-ERK 1 and 2, respectively) compared with mock-transfected, vehicle-treated cells (Fig. 5). MTX treatment further increased the phosphorylation levels of these two proteins by 4 and 7 fold, while decreasing their total levels. Quantitative RT-PCR revealed that silencing of c-Myc expression alone did not alter ERK1 transcription (reduction of 13%). In contrast, its combination with MTX reduced transcription of ERK1 by 54% compared with mock-transfected, vehicle-treated cells, which could be an explanation for the reduced total ERK levels found by immunoblot. Nevertheless, c-Myc expression was found almost completely down-regulated (reduction of 90%) (Fig. 5), which was similar to the simultaneous treatment of MTX and U0126 in non-transfected vehicle-treated A549 cells (Fig. 2B). In parallel,

MTX significantly increased gelsolin expression by about four fold and decreased SP-A levels nearly by 70%, compared with mock-transfected A549 cells (Fig. 5). Moreover, as shown in Figure 6, detection of the epithelial marker cytokeratin by immunocytochemistry highlighted that the majority of A549 cells transfected with siRNA c-Myc showed differentiated morphology to normal epithelial cells under MTX treatment (Fig. 6F). In contrast, MTX alone only induced differentiation in a very low percentage of non-transfected A549 cells (Fig. 6B), whereas its combination with U0126 enhanced this effect, inducing differentiation in practically all A549 cells (Fig. 6D). Together, these results confirm that ERK-stabilized c-Myc protein expression plays a central role in the resistance of arrested A549 cells to MTX-induced differentiation. The cell proliferation rate after withdrawal of these compounds at the end of treatment was studied in order to investigate whether the differentiation provoked by the simultaneously combination of antimetabolites and U0126 was irreversible. A549 cells treated with both antimetabolites or U0126 alone for 96 h showed increased cell number after drug withdrawal in a similar time-dependent manner to (U0126 and MTX 0.1 μ M; Fig. 7A) or somewhat slower as (MTX 10 μ M and GE; Fig. 7B, C, D) control cells. This indicates that they relatively quickly regained their neoplastic properties after antimetabolite treatment. In contrast, cells treated simultaneously with MTX (10 μ M) or GE plus U0126 preserved their epithelial-like phenotype and did not show an increase in number even three weeks after end of treatment (Fig. 7B, C and D).

DISCUSSION

After short- (24 h) and long-time (96 h) treatment with the antimetabolites MTX and GE the majority of A549 cells were found in a non-proliferative phase of the cell cycle (i.e., G₀/G₁), although only very few of them changed their morphology to an epithelial-like cell phenotype during long-time treatment. This fact was corroborated by the modulation of several proteins involved in differentiation. The general differentiation marker gelsolin, an actin regulatory protein, shows decreased expression in lung cancers compared with histologically normal surrounding lung tissue (Dosaka-Akita et al., 1998). In non-small cell lung cancer (NSCLC) cells its expression can be augmented *in vitro* by differentiation inducers, such as agonists of the peroxisome proliferator-activated receptor γ (Chang and Szabo, 2000), and this increase correlates with inhibition of cell growth (Jarrard et al., 1998). On the other hand, SP-A and SP-C proteins are specific markers for undifferentiated progenitor cells for lung alveolar epithelium (i.e. type II pneumocytes) and produced in high quantity during repair of injury and carcinogenesis by these cells (Betz et al., 1995; Broers et al., 1992). Consequently, their cellular levels are significantly reduced during differentiation of lung adenocarcinoma cells in the presence of various differentiation inducers (Jarrard et al., 1998; Chang et al., 2000). In this sense, the observed up-regulation of gelsolin and the down-regulation of SP-A and SP-C levels in MTX- and GE-treated A549 cells underline a cellular tendency to differentiate away from the progenitor type II pneumocytes to a less malignant phenotype and confirm the general potential of both antimetabolites to induce the differentiation process. Indeed, the morphologically changed cells showed a drastic reorganization of cytokeratin (Fig. 6), and appeared epithelial cell-like.

Paradoxically, the antiproliferative effect of MTX and GE in A549 cells was accompanied by a sustained activation of the ERK1/2 pathway, which one would rather expect to be deactivated under growth arrest conditions. This observation, together with the fact that both antitumoral compounds were generally able to induce differentiation in a small percentage of cells, suggested that sustained ERK1/2 activation might be an antitumoral resistant mechanism in A549 cells, counteracting the differentiation process. In fact, inhibition of MTX- and GE-induced sustained ERK1/2 phosphorylation by the specific MEK inhibitor U0126 provoked differentiation to an epithelial-like cell phenotype in practically all cells. This event was reflected by: i) a three fold increased expression of the general differentiation marker gelsolin, together with a further decrease of SP-A and SP-C levels, compared to MTX and GE alone, ii) the induction of cytoplasmatic multilamellar bodies (myelinosomes), typical secretory granules present in differentiated type II alveolar cells, which were hardly generated by MTX alone, and finally iii) the reorganization of the differentiation marker cytokeratin in all cells. Interestingly, administration of the specific MEK inhibitor alone, neither changed the levels of the mentioned specific differentiation markers nor induced differentiation in any of the cells. This clearly demonstrates that suppression of ERK1/2 phosphorylation is not a general key to inducing differentiation in A549 cells, but that sustained over-activation of this pathway must be considered a resistance mechanism to the differentiation potential of MTX and GE. Accordingly, Singh and coworkers have recently demonstrated that MTX is able to induce differentiation in a small percentage of colon cancer cells, and that inhibition of the MAPK/ERK pathway in combination with MTX also enhanced the amount of differentiation in these cells (Singh et al., 2006).

Besides the sustained ERK1/2 phosphorylation, we detected a down-regulation of c-Myc protein expression under MTX and GE treatment, which was nearly complete^[MSOffice5] by the simultaneous administration of the inhibitor U0126 (Fig. 2B). The c-myc proto-oncogene encodes the nuclear transcription factor c-Myc that is crucially involved in cell-fate decisions, including proliferation, apoptosis and cell differentiation (Henriksson and Luscher, 1996). Deregulated c-Myc expression is implicated in the development of a wide spectrum of human cancers, and c-Myc has therefore been proposed as molecular target for cancer treatment (Vita and Henriksson, 2006). Accordingly, overexpression of c-Myc is observed in NSCLC (Gazzeri et al., 1991; Lorenz et al., 1994), and suppression of c-Myc expression appears to be necessary for differentiation of hepatocellular carcinomas in normal appearing liver cells (Shachaf et al., 2004). Thus, reduction of total c-Myc levels in A549 cells treated with MTX or GE alone could, in part, explain the inhibition of growth and the modulation of differentiation markers, demonstrating that these chemotherapeutic antimetabolites are generally able to trigger differentiation in these cells. The exact mechanisms by which these drugs are able to lower c-Myc levels in A549 cells have not yet been clarified. Chu and coworkers have demonstrated that thymidylate synthase (TS), an enzyme involved in the *de novo* biosynthesis of the pyrimidine 2'-deoxyribonucleotide thymidine monophosphate (dTMP), directly interacts with the c-myc mRNA in human colon cancer cells, thereby inhibiting its translational efficiency (Chu et al., 1995). Moreover, TS levels are regulated by its own product through a negative autoregulatory mechanism. Therefore, it might be possible that inhibition of dihydrofolate reductase and TS by MTX (Kimura et al., 2004; McGuire, 2003), disturbs the expression of c-Myc by the sequestration of its mRNA in A549 cells through depletion of intracellular dTMP and consequently increased TS levels. On the other

hand, MTX and GE also interfere in the metabolism of nucleotides (i.e., ATP and GTP), which, besides DNA synthesis, also participate in the regulation of other important cellular functions, such as protein synthesis, signal transduction via GTP-binding proteins, cAMP synthesis, among others. Hence, a relatively small variation of these nucleotide pools may have a critical impact on the global regulation of cell growth and differentiation by modulating the activity of key signal transduction pathways and proteins involved in these cellular events, as shown in other cancer cells (Bierau et al., 2006; Singh et al., 2006).

Accordingly, it has been shown that ERK pathway activation can enhance c-Myc protein stability through phosphorylation of Serine 62 by activated ERK1/2, blocking its proteasome-mediated degradation (Lutterbach and Hann, 1994). The role of c-Myc in counteracting the effect of MTX in our cell system was further substantiated by demonstrating that transient inactivation of c-Myc expression with the corresponding siRNA allowed MTX alone, independently of the status of ERK1/2 phosphorylation, to induce differentiation in a similar manner and extent as shown by the simultaneous combination of MTX and U0126 (Fig. 5 and 6). Thus, down-regulation of c-Myc levels seems to be the key regulator addressed by the sustained phosphorylated ERK pathway. However, c-Myc inactivation alone by siRNA in the absence of MTX did not initiate this process. It is noteworthy that our results contrast to the prevalent opinion that ERK1/2 activation is always associated with cell proliferation or differentiation, including in A549 cells (Keshamouni et al., 2004). Silencing of c-Myc expression in the presence of MTX decreased ERK1 transcription, being a possible explanation for the reduced total ERK1 levels shown by immunoblot (Fig. 5). Increasing phosphorylation levels of ERK while reducing total protein levels are not necessarily contradictory. Since only a small fraction of total ERK is normally phosphorylated, this fraction might

increase even when total ERK levels decrease. It is important to note that ERK phosphorylation in cells transfected with siRNA c-Myc and treated with MTX was about 5 fold higher than it could be induced by treatment of non-transfected cells with MTX plus U0126. It might be possible that ERK transcription is inhibited in response to its sustained phosphorylation as a consequence of the complete down-regulation of c-Myc expression induced by combination of silencing c-Myc and MTX. Moreover, we can not exclude that this excessive sustained phosphorylation also induced a degradation process of total ERK levels over time.

The most important result perhaps is the fact that once A549 cells were differentiated by MTX or GE plus U0126, they neither proliferated nor reverted their morphological appearance after withdrawal of the compounds. This demonstrates that, in contrast to MTX, GE or U0126 alone, only deactivation of the ERK1/2 pathway during antimetabolite treatment was able to induce an irreversible and permanent differentiation state of these cells.

Our work demonstrates that non-small cell lung cancer cells preserve their capacity to revert into a permanently differentiated phenotype under long-term chemotherapeutic treatment with the antimetabolites MTX and GE. Furthermore, our results reveal that the maintenance of a certain threshold of c-Myc expression through sustained ERK1/2 activation represents the molecular mechanism that confers resistance to MTX- and GE-induced cell differentiation in A549 cells. In the light of these findings, sustained ERK1/2 activation might represent a general resistance mechanism for tumoral cells to avoid differentiation during MTX or similar chemotherapeutic drugs. Moreover, it could be possible to combine MTX, GE or other antimetabolites with drugs able to inhibit, directly or indirectly, the MAPK ERK pathway or c-Myc, such as antitumoral tyrosine-kinase inhibitors. Taken together, these data provide a

novel molecular basis for therapeutic strategies based on irreversible differentiation of cancer cells using conventional chemotherapeutic antimetabolites in combination with inhibitors of the MEK/ERK pathway or c-Myc.

REFERENCES

- Betz C, Papadopoulos T, Buchwald J, Dammrich J and Muller-Hermelink HK (1995) Surfactant protein gene expression in metastatic and micrometastatic pulmonary adenocarcinomas and other non-small cell lung carcinomas: detection by reverse transcriptase-polymerase chain reaction. *Cancer Res* **55**:4283-4286.
- Bierau J, van Gennip AH, Rutger Meinsma RL, Caron HN, van Kuilenburg ABP (2006) Cyclopentenyl cytosine-induced activation of deoxycytidine kinase increases gemcitabine anabolism and cytotoxicity in neuroblastoma. *Cancer Chemother Pharmacol* **57**:105-113.
- Broers JL, Jensen SM, Travis WD, Pass H, Whitsett JA, Singh G, Katyal SL, Gazdar AF, Minna JD and Linnoila RI (1992) Expression of surfactant associated protein-A and Clara cell 10 kilodalton mRNA in neoplastic and non-neoplastic human lung tissue as detected by in situ hybridization. *Lab Invest* **66**:337-346.
- Chang TH and Szabo E (2000) Induction of differentiation and apoptosis by ligands of peroxisome proliferator-activated receptor gamma in non-small cell lung cancer. *Cancer Res* **60**:1129-1138.
- Chen JP, Chen L, Leek J and Lin C (2006) Antisense c-myc fragments induce normal differentiation cycles in HL-60 cells. *Eur J Clin Invest* **36**:49-57.
- Chu E, Takechi T, Jones KL, Voeller DM, Copur SM, Maley GF, Maley F, Segal S and Allegra CJ (1995) Thymidylate synthase binds to c-myc RNA in human colon cancer cells and in vitro. *Mol Cell Biol* **15**:179-185.
- d'Amato TA, Landreneau RJ, Ricketts W, Huang W, Parker R, Mechetner E, Yu IR, Luketich JD (2007) Chemotherapy resistance and oncogene expression in non-small cell lung cancer. *J Thorac Cardiovasc Surg* **133**:352-359.

- Dosaka-Akita H, Hommura F, Fujita H, Kinoshita I, Nishi M, Morikawa T, Katoh H, Kawakami Y and Kuzumaki N (1998) Frequent loss of gelsolin expression in non-small cell lung cancers of heavy smokers. *Cancer Res* **58**:322-327.
- Gazzeri S, Brambilla E, Jacrot M, Chauvin C, Benabid AL and Brambilla C (1991) Activation of myc gene family in human lung carcinomas and during heterotransplantation into nude mice. *Cancer Res* **51**:2566-2571.
- Henriksson M and Luscher B (1996) Proteins of the Myc network: essential regulators of cell growth and differentiation. *Adv Cancer Res* **68**:109-182.
- Hoshikawa Y, Kwon HJ, Yoshida M, Horinouchi S and Beppu T (1994) Trichostatin A induces morphological changes and gelsolin expression by inhibiting histone deacetylase in human carcinoma cell lines. *Exp Cell Res* **214**:189-197.
- Jarrard JA, Linnoila RI, Lee H, Steinberg SM, Witschi H and Szabo E (1998) MUC1 is a novel marker for the type II pneumocyte lineage during lung carcinogenesis. *Cancer Res* **58**:5582-5589.
- Keshamouni VG, Reddy RC, Arenberg DA, Joel B, Thannickal VJ, Kalemkerian GP and Standiford TJ (2004) Peroxisome proliferator-activated receptor-gamma activation inhibits tumor progression in non-small-cell lung cancer. *Oncogene* **23**:100-108.
- Kimura E, Nishimura K, Sakata K, Oga S, Kashiwagi K and Igarashi K (2004) Methotrexate differentially affects growth of suspension and adherent cells. *Int J Biochem Cell Biol* **36**:814-825.
- Kohno M and Pouyssegur J (2006) Targeting the ERK signaling pathway in cancer therapy. *Ann Med* **38**:200-211.

- Lorenz J, Friedberg T, Paulus R, Oesch F and Ferlinz R (1994) Oncogene overexpression in non-small-cell lung cancer tissue: prevalence and clinicopathological significance. *Clin Investig* **72**:156-163.
- Lutterbach B and Hann SR (1994) Hierarchical phosphorylation at N-terminal transformation-sensitive sites in c-Myc protein is regulated by mitogens and in mitosis. *Mol Cell Biol* **14**:5510-5522.
- Maghfoor I and Perry MC (2005) Lung cancer. *Ann Saudi Med* **25**:1-12.
- Marchal JA, Rodriguez-Serrano F, Campos J, Madeddu R, Boulaiz H, Martinez-Amat A, Carrillo E, Caba O, Prados JC, Velez C, Melguizo C, Montella A and Aranega A (2006) Differentiation: an encouraging approach to anticancer therapy. *Ital J Anat Embryol* **111**:45-64.
- Martinez J, Gutierrez A, Casas J, Llado V, Lopez-Bellan A, Besalduch J, Dopazo A and Escriba PV (2005a) The repression of E2F-1 is critical for the activity of Minerval against cancer. *J Pharmacol Exp Ther* **315**:466-474.
- Martinez J, Vogler O, Casas J, Barcelo F, Alemany R, Prades J, Nagy T, Baamonde C, Kasprzyk PG, Teres S, Saus C and Escriba PV (2005b) Membrane structure modulation, protein kinase C alpha activation, and anticancer activity of minerval. *Mol Pharmacol* **67**:531-540.
- McGuire JJ (2003) Anticancer antifolates: current status and future directions. *Curr Pharm Des* **9**:2593-2613.
- Moran CA (2006) Pulmonary adenocarcinoma: the expanding spectrum of histologic variants. *Arch Pathol Lab Med* **130**:958-962.
- Nishimoto S and Nishida E (2006) MAPK signalling: ERK5 versus ERK1/2. *EMBO Rep* **7**:782-786.
- Seger R and Krebs EG (1995) The MAPK signaling cascade. *Faseb J* **9**:726-735.

- Shachaf CM, Kopelman AM, Arvanitis C, Karlsson A, Beer S, Mandl S, Bachmann MH, Borowsky AD, Ruebner B, Cardiff RD, Yang Q, Bishop JM, Contag CH and Felsher DW (2004) MYC inactivation uncovers pluripotent differentiation and tumour dormancy in hepatocellular cancer. *Nature* **431**:1112-1117.
- Singh R, Fouladi-Nashta AA, Li D, Halliday N, Barrett DA and Sinclair KD (2006) Methotrexate induced differentiation in colon cancer cells is primarily due to purine deprivation. *J Cell Biochem* **99**:146-155.
- Spira AI and Carducci MA (2003) Differentiation therapy. *Curr Opin Pharmacol* **3**:338-343.
- Vita M and Henriksson M (2006) The Myc oncoprotein as a therapeutic target for human cancer. *Semin Cancer Biol* **16**:318-330.

FOOTNOTES

This work was supported by Grants “Nous estudis immunogenotípics en la classificació i tractament de la LMA i SMD” and PROGECIB-8A (Conselleria d’Economia, Hisenda i Innovació, Govern Balear). The Dorothy & Jim Bird Foundation also provided funds for this study. Jordi M. Serra and Antonio Gutiérrez contributed equally to this work. Regina Alemany and Oliver Vögler are supported by the Spanish I3 Programme (“Programa de Incentivación de la Incorporación e Intensificación de la Actividad Investigadora”).

FIGURE LEGENDS

Figure 1. Methotrexate inhibits cell proliferation by impairing cell cycle progression through the G1 checkpoint. DNA content of A549 cells was measured by flow cytometry. Histograms of vehicle- (control) (A) and methotrexate- (MTX) treated cells (10 μ M) (B) for 24 h are shown. The fluorescence values used to calculate the peaks corresponding to the G0/G1 and the G2/S/M phase are indicated on each histogram. C) The percentage of cells in G0/G1 and S/G2/M phase with respect to the total cell number after 24 h in the absence (control) or presence of MTX (10 μ M). The data are the mean \pm S.E.M. values of three independent experiments. * P <0.001. D) Immunodetection of PARP fragmentation in A549 cells incubated in the absence (C) or presence of MTX (1 and 10 μ M) for 24 h, and a positive control of apoptosis (C+, cisplatin 1 μ M).

Figure 2. A) Methotrexate induces sustained phosphorylation of ERK1/2 without affecting total ERK levels. A549 cells were treated with 1 or 10 μ M methotrexate (MTX) for 24 h (upper panel) and 96 h (middle and lower panels). **B) Inhibition of the MEK/ERK pathway reduces basal and antimetabolite-induced ERK1/2 phosphorylation and down-regulates c-Myc protein levels.** A549 cells were treated with vehicle, MTX (10 μ M), gemcitabine (GE) (1 μ M) and the MEK inhibitor U0126 (U0) (10 μ M) separately or in combination for 96 h. Levels of phosphorylated ERK1/2, total ERK1/2 and total c-Myc proteins were quantified against standard curves and normalized to the protein content of vehicle-treated cells (control, C) (taken as 100%). Immunoreactive bands are representative of five independent experiments.

Figure 3. Methotrexate and gemcitabine in combination with ERK1/2 inhibition enhance modulation of differentiation markers. A549 cells were treated with vehicle, U0126 (10 μ M), methotrexate (MTX) (10 μ M), gemcitabine (GE) (1 μ M) and MTX or GE plus U0126 for 96 h. Insets show representative immunoblots of gelsolin (A), SP-A (B) and SP-C (C) of five independent experiments. Columns show levels (means \pm S.E.M.) of gelsolin (A), SP-A (B) and SP-C (C) quantified against standard curves and normalized to the protein content of vehicle-treated cells (control) (taken as 100%). ** $P < 0.01$ and *** $P < 0.001$ vs control; # $P < 0.05$ and ## $P < 0.01$ vs MTX- or GE-treated cells (One-way Anova followed by Tukey's comparison test).

Figure 4. Methotrexate in combination with ERK1/2 inhibition induces cytoplasmatic multilamellar bodies (myelinosomes) appearance. A549 cells were treated with vehicle (A), methotrexate (MTX) (10 μ M) (B) or MTX plus U0126 (C) for 96 h, fixed in 4% glutaraldehyde and processed for electron microscopy. The presence of multilamellar bodies (MLB) (arrows) was particularly evident only in cells treated simultaneously with MTX and the MEK inhibitor U0126 (C), compared with vehicle- (A) and MTX-treated cells (B). Magnification: Upper panels 5000 fold; lower panels 15000 fold. Bars = 5 μ m or 15 μ m, respectively.

Figure 5. Silencing of c-Myc expression enables methotrexate alone to induce differentiation. A549 cells were transfected with validated siRNA targeting human c-Myc mRNA (5 nM). 48 h after transfection, vehicle (control, C) or methotrexate (MTX) (10 μ M) was added to the cells and incubated for additional 96 h. Levels of c-Myc, phosphorylated ERK1/2, total ERK1/2, gelsolin and SP-A proteins were quantified against standard curves and normalized to the protein content of control cells (taken as

100%). Immunoreactive bands are representative of five independent experiments. No variation could be detected in mock-transfected (control) compared to non-transfected cells.

Figure 6. Methotrexate in combination with ERK1/2 inhibition or c-Myc silencing induces ubiquitous cellular differentiation. A549 cells were treated with vehicle (A), methotrexate (MTX) (10 μ M) (B), U0126 (10 μ M) (C), MTX plus U0126 (D) for 96 h or transfected with siRNA c-Myc for 48 h and then treated additionally with vehicle (E) or MTX (10 μ M) (F) for 96 h. Detection of the intermediate filament protein cytokeratine was performed by immunocytochemistry. MTX in combination with U0126 (D) in non-transfected cells or MTX alone in cells transfected with siRNA c-Myc (F) provoked ubiquitous cellular reorganization of cytokeratine, increase in cell size, and increased cytoplasmatic:nuclear ratio compared to MTX (B) or U0126 (C) alone in non-transfected cells or to vehicle-treated siRNA c-Myc-transfected cells (E), respectively. All pictures are taken with the same magnification: 200 fold (insets 800 fold).

Figure 7. Irreversible differentiation of A549 cells by simultaneous treatment with methotrexate and gemcitabine plus U0126. A549 cells were treated with vehicle, U0126 (10 μ M) (A), methotrexate (MTX) (0.1 and 10 μ M) (A and B), gemcitabine (GE) (0.1 and 1 μ M) (C and D) alone and MTX or GE plus U0126 for 96 h (A-D). Cells were then recovered, diluted and replated at a density of 10 cells per well in 24-well plates with 0.5 ml of culture medium without any further compounds. After ten and twenty days cells were counted using an automated cell counter. Values are means \pm S.E.M. of three independent experiments.

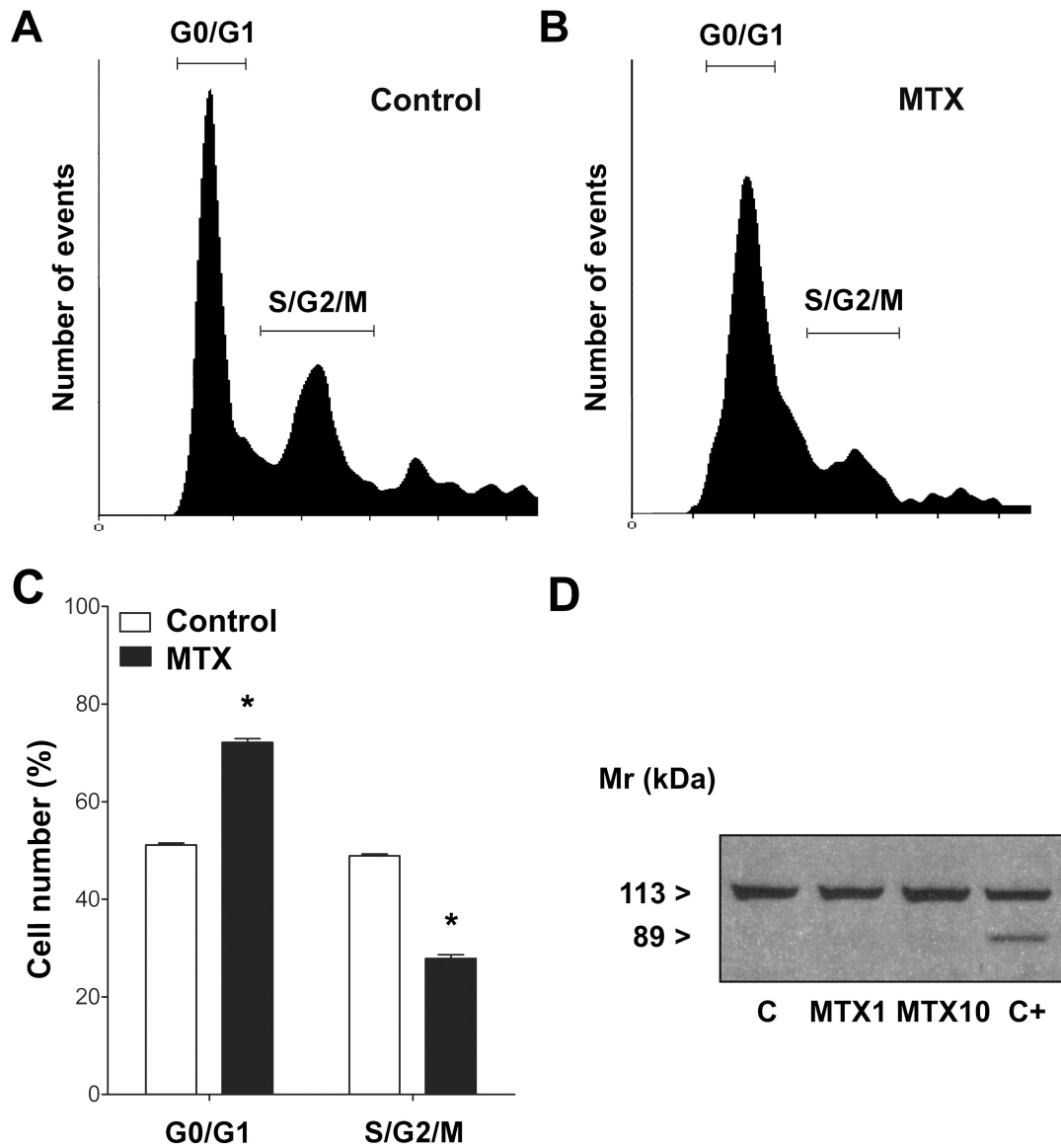


Figure 1

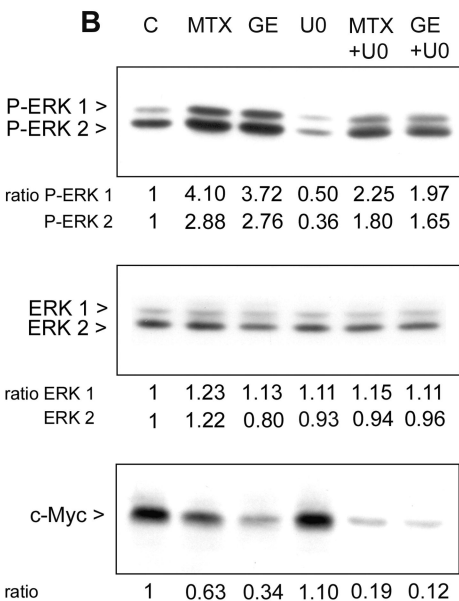
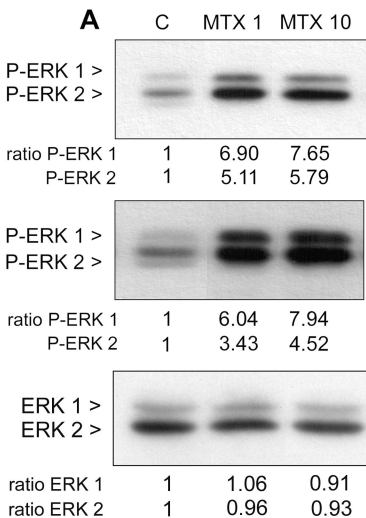


Figure 2

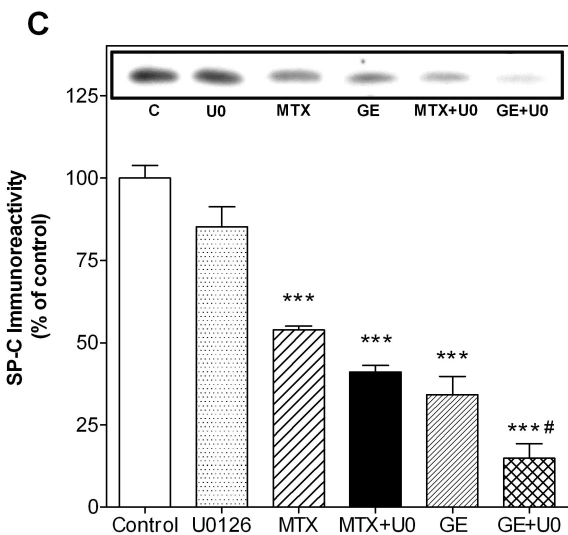
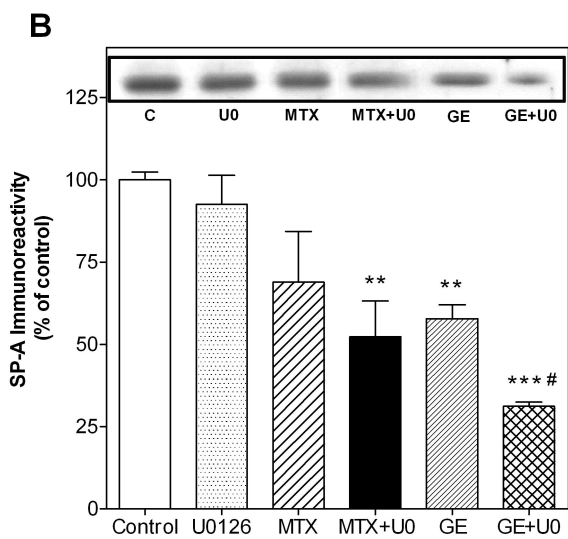
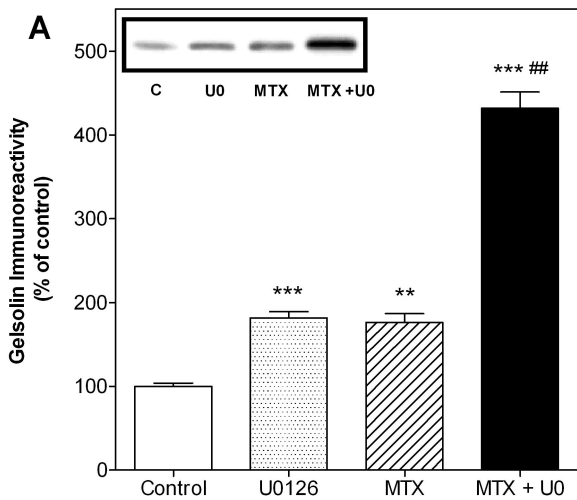


Figure 3

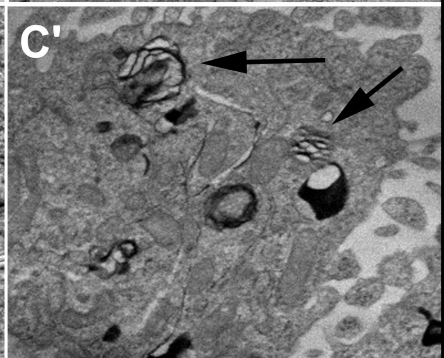
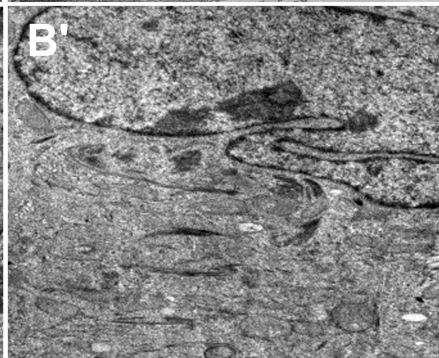
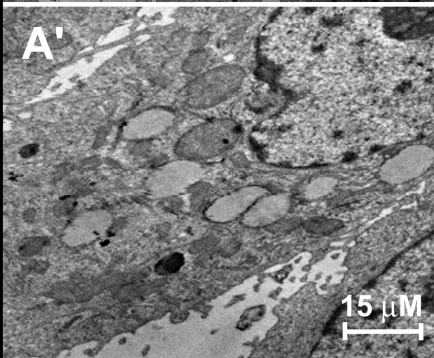
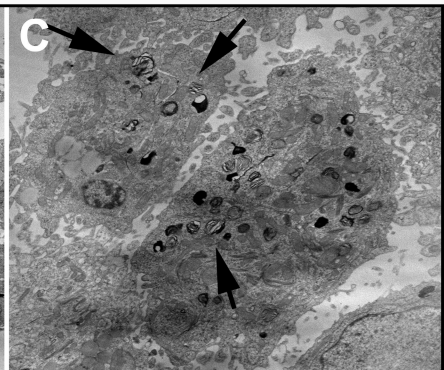
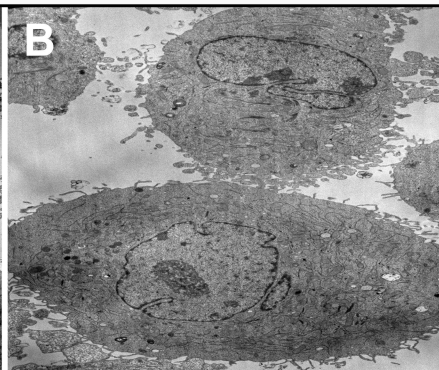
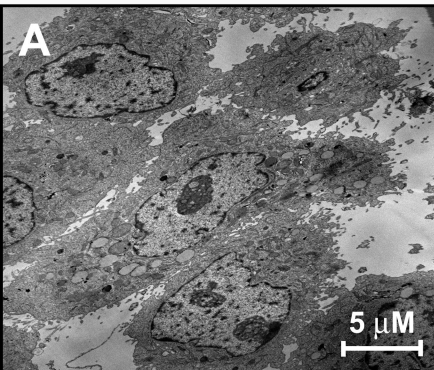


Figure 4

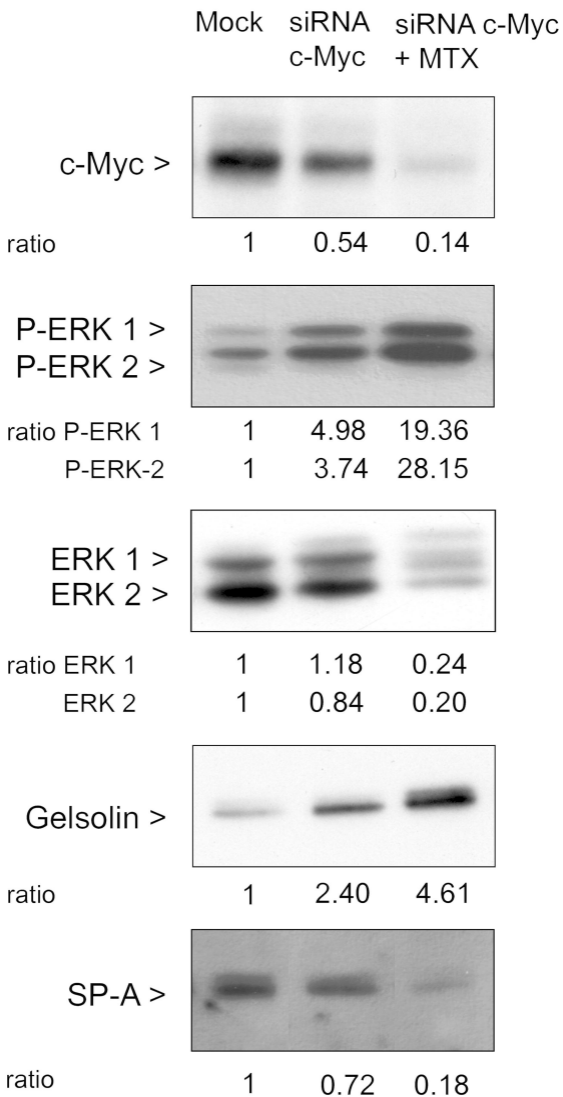


Figure 5

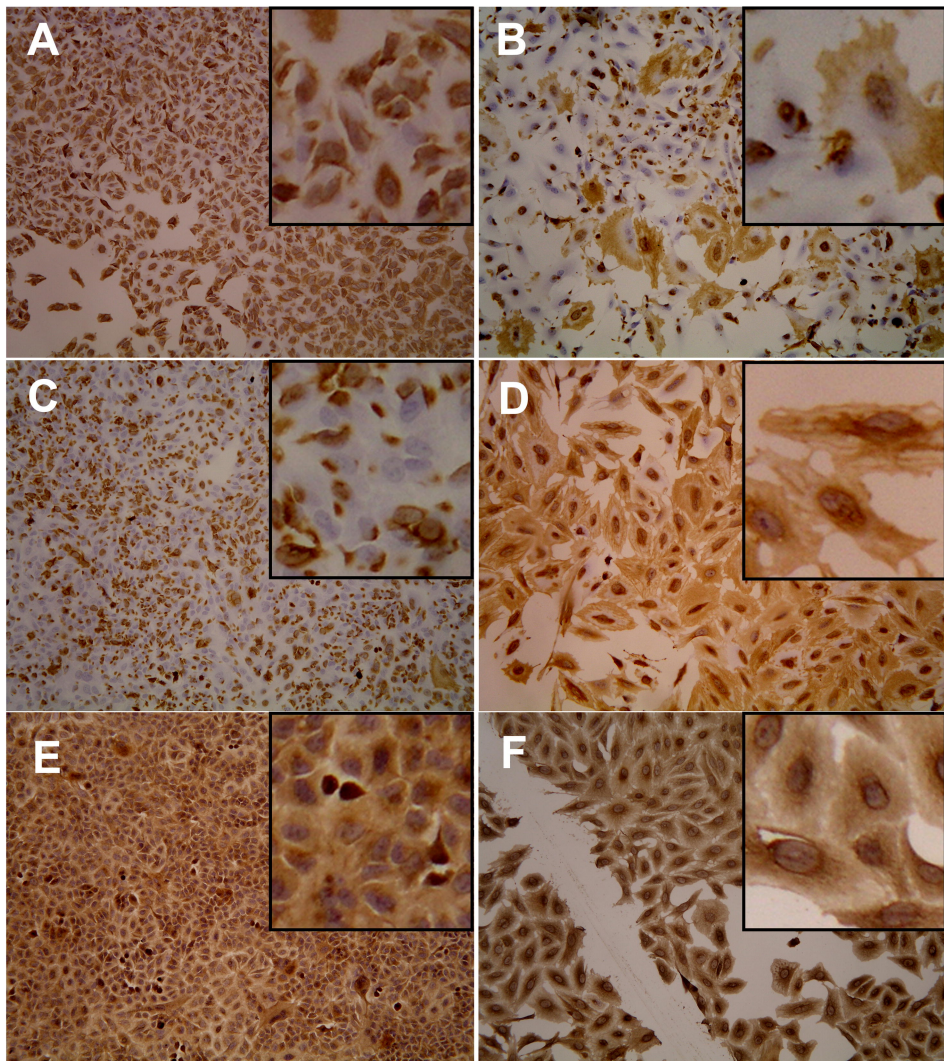


Figure 6

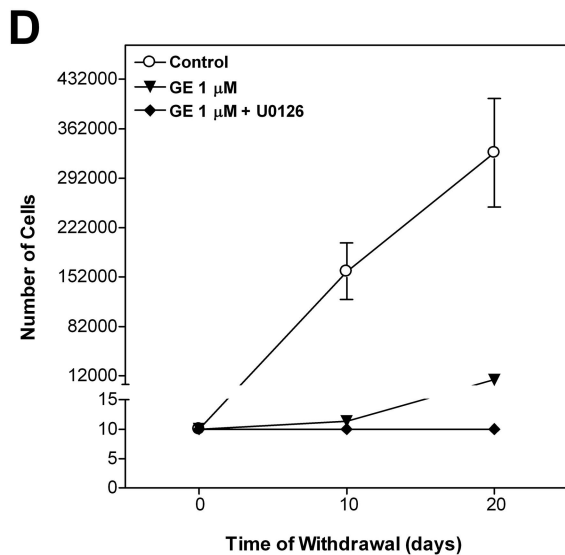
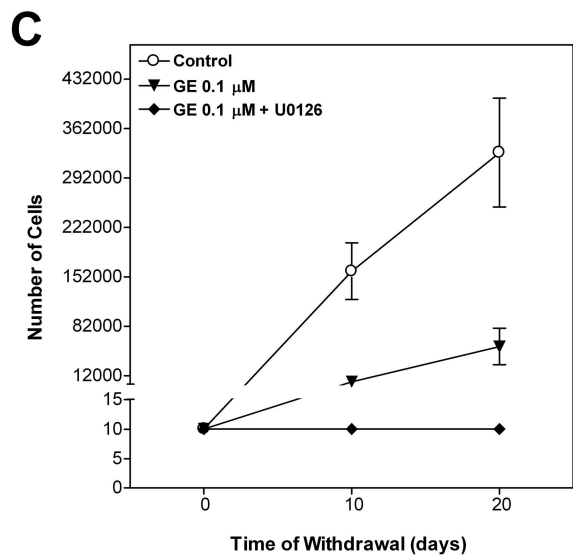
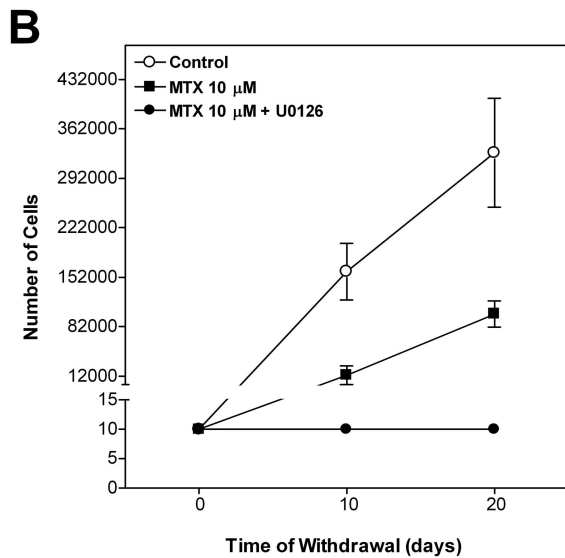
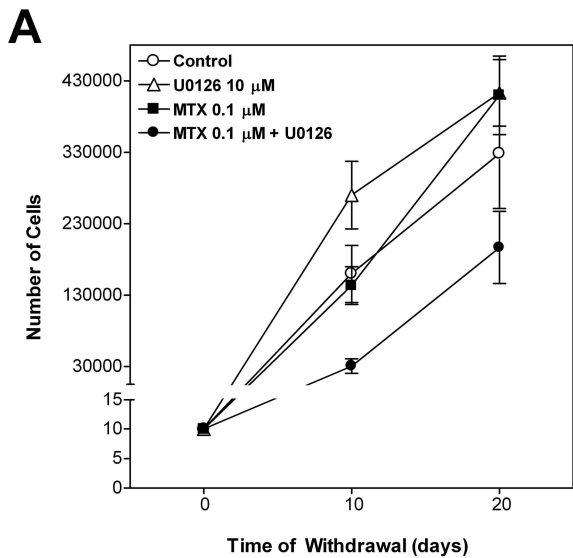


Figure 7